White Matter-Governed Superior Frontal Sulcus Surgical Paradigm: A Radioanatomic Microsurgical Study—Part I

Alejandro Monroy-Sosa, MD*
Srikant S. Chakravarthi, MD, MSc*
Melanie B. Fukui, MD*
Bhavani Kura, MD*
Jonathan E. Jennings, MD*
Juanita M. Celix, MD, MPH*
Kenneth C. Nash, MD‡
Mikaeel Kassam*§
Richard A. Rovin, MD*
Amin B. Kassam, MD*§

*Department of Neurosurgery, Aurora Neuroscience Innovation Institute, Aurora St. Luke's Medical Center, Milwaukee, Wisconsin; ‡Department of Psychiatry, University of Pittsburgh Medical Center, Pittsburgh, Pennsylvania; §Neeka Health, Milwaukee, Wisconsin

Correspondence:
Amin B. Kassam, MD,
Aurora St. Luke's Medical Center,
Suite 630,
2801 W Kinnickinnic River Pkwy,
Milwaukee, WI 53215, USA.
Email: amin.kassam@aurora.org

Received, April 25, 2019.
Accepted, January 13, 2020.

BACKGROUND: Frontal subcortical and intraventricular pathologies are traditionally accessed via transcortical or interhemispheric-transcallosal corridors.

OBJECTIVE: To describe the microsurgical subcortical anatomy of the superior frontal sulcus (SFS) corridor.

METHODS: Cadaveric dissections were undertaken and correlated with magnetic resonance imaging/diffusion-tensor imaging-Tractography. Surgical cases demonstrated clinical applicability.

RESULTS: SFS was divided into the following divisions: proximal, precentral sulcus to coronal suture; middle, 3-cm anterior to coronal suture; and distal, middle division to the orbital crest. Anatomy was organized as layered circumferential rings projecting radially towards the ventricles: (1) outer ring: at the level of the SFS, the following lengths were measured: (A) precentral sulcus to coronal suture = 2.29 cm, (B) frontal bone projection of superior sagittal sinus (SSS) to SFS = 2.37 cm, (C) superior temporal line to SFS = 3.0 cm, and (D) orbital crest to distal part of SFS = 2.32 cm; and (2) inner ring: (a) medial to SFS, U-fibers, frontal aslant tract (FAT), superior longitudinal fasciculus I (SLF-I), and cingulum bundle, (b) lateral to SFS, U-fibers, (SLF-II), claustrocortical fibers (CCF), and inferior fronto-occipital fasciculus, and (c) intervening fibers, FAT, corona radiata, and CCF. The preferred SFS parafascicular entry point (SFSP-EP) also referred to as the Kassam-Monroy entry point (KM-EP) bisects the distance between the midpupillary line and the SSS and has the following coordinates: x = 2.3 cm (lateral to SSS), y ≥ 3.5 cm (anterior to CS), and z = parallel corona radiata and anterior limb of the internal capsule.

CONCLUSION: SFS corridor can be divided into lateral, medial, and intervening white matter tract segments. Based on morphometric assessment, the optimal SFSP-EP is y ≥ 3.5 cm, x = 2.3 cm, and z = parallel to corona radiata and anterior limb of the internal capsule.

KEY WORDS: Superior frontal sulcus (SFS), Transsulcal, Parafascicular, Port, Intraventricular, White matter tract (WMT), Lateral ventricle

Operative Neurosurgery 0:1–14, 2020 DOI: 10.1093/ons/opaa065

Surgical access to frontal subcortical, intra-axial, and intraventricular pathology has primarily been accomplished via either transcortical or transcallosal routes. The early transsulcal work of Patrick Kelly and Gazi Yasargil,[1-4] in an effort to preserve white

ABBREVIATIONS: 3D, three-dimensional; **CCF,** claustrocortical fibers; **DTI,** diffusion-tensor imaging; **EP,** entry point; **FAT,** frontal aslant tract; **ICRC,** inner circumferential-radial corridor; **IFOF,** inferior fronto-occipital fasciculus; **KM-EP,** Kassam-Monroy entry point; **MRI,** magnetic resonance imaging; **OCRC,** outer circumferential-radial corridor; **SFS,** superior frontal sulcus; **SFS-DD,** SFS-Distal division; **SFS-MD,** SFS-Middle division; **SFS-PD,** SFS-Proximal division; **SFSP-EP,** SFS parafascicular entry point; **SLF,** superior longitudinal fasciculus; **SMA,** supplementary motor area; **SSS,** superior sagittal sinus; **TPCS,** transsulcal parafascicular corridor surgery; **WMTs,** white matter tracts

Supplemental digital content is available for this article at www.operativeneurosurgery-online.com.

matter tracts (WMTs) and reduce cortical iatrogenic injury, led to the evolution of transsulcal parafascicular corridor surgery (TPCS).[5-15]

Building on the concept of tailored TPCS, through microsurgical anatomy, we report a transsulcal-parafascicular approach to the frontal horn, third ventricle, and subcortical frontal lobe. As a part of the customization of TPCS, respective divisions of the superior frontal sulcus (SFS) are used for entry.[6,16,17]

Objectives

Three primary study objectives included:

I. Describe SFS complex relative to key anatomic landmarks (bone, vessels, gyri, sulci, WMTs, and ventricles);
II. Correlate SFS corridor with magnetic resonance imaging (MRI)-DTI using 3-dimensional (3D) computer simulation; and
III. Describe 2 clinical case examples demonstrating feasibility.

METHODS

Neuroanatomical Study

Five embalmed cadaveric specimens (10 hemispheres) injected with red-blue silicon were frozen (2 wk at −15°C) and prepared as previously described.[18-23] Osseous landmarks (ie, superior temporal line, orbital crest, coronal, and the frontal bone projection of the superior sagittal sinus (SSS) were analyzed in relationship to SFS. Length and depth of SFS was measured with digital calipers (Vernier Software & Technology, Beaverton, Oregon). Morphology and divisions of SFS were described based on anatomic-surgical perspectives.

The surgical corridor surrounding SFS was sequentially exposed and divided into 2 circumferential rings progressively encountered as the surgeon travels from the surface to the depth radially towards the ventricles: (1) the outer circumferential-radial corridor (OCRC) consisted of osseous, gyral, sulcal, and vascular landmarks, and (2) the inner circumferential-radial corridor (ICRC) consisted of WMTs and the ventricles (Figure 1).

The BrainPath portal access device (NICO Corporation, Indianapolis, Indiana) was used to simulate the SFS parafascicular entry point (SFSP-EP), also referred to as the Kassam-Monroy entry point (KM-EP) and the trajectory.

Neuroradiological Correlation Using 3D Computational Simulation

Tracts were manually segmented, and 3D-tractography data were generated using an FDA-approved surgical planning software (BrightMatter™ Plan, Synaptive Medical, Toronto, Canada).

Clinical Application and Feasibility of the Corridor

We provide 2 case examples: (1) a colloid cyst and (2) a large central neurocytoma. This portion of the study was approved by the Institutional Review Board (16-37MR). Consent was obtained from all patients.

We specifically selected a commonly encountered, as well as complex, pathology demonstrating the broad feasibility of KM-EP via TPCS.

RESULTS

Microsurgical Cadaveric Study

The Outer Ring

Outer circumferential-radial corridor:

(a) Osseous: Coronal suture is the fiduciary bony landmark separating SFS into 2 of its 3 constituents: the proximal and middle divisions. In the sagittal plane/anterior-posterior that we define as the y-axis, the length from the precentral sulcus to the coronal suture was 2.29 cm. The middle division extends 3 cm anterior to coronal suture. Finally, the distal division then continues from the middle division at a length of 3.5 cm to the orbital crest (Figures 1 and 2).

In the coronal plane/lateral that we define as the x-axis, the SFS was 2.37 cm lateral to SSS; alternatively, SFS can be located 3.0 cm medial to superior temporal line (Figures 1 and 2).

(b) Sulcal topography: SFS, the precentral sulcus, separates the precentral gyrus and the superior frontal gyrus. The SFS starts orthogonally at the precentral sulcus and runs parallel to the interhemispheric fissure towards the frontal pole.

The SFS complex is divided into 3 divisions (Figure 2, Table 1 and 2):

(i) SFS proximal division (SFS-PD) extends from precentral sulcus to coronal suture;
(ii) SFS middle division (SFS-MD) extends 3.0 cm anterior to coronal suture; and
(iii) SFS distal division (SFS-DD) extends from the distal end of SFS-MD to orbital crest. Near the frontal pole, this division branches into several short sulci, referred to as "accessory SFS," which occupy the most distal division and contribute to an additional 2.0 cm of SFS-DD.

The SFS was continuous in 2/5 (40%) and interrupted in 3/5 (60%) of specimens. Interruption was most prominent in SFS-PD and SFS-MD, wherein the presence of the gyral bridge crossing the SFS was observed in 2/5 (40%) and 1/5 (20%), respectively. Mean length and depth of SFS was 7.32 and 1.84 cm, respectively (Figure 2).

(c) Vasculature: Arteries in the OCRC are the precentral and prefrontal arteries and the anterior, middle, and posterior internal frontal arteries; veins are middle frontal, posterior frontal, and precentral veins (Figure 2).
(d) Cortical gyri: SFS separates the superior and middle frontal gyrus. A face-to-face mirrored relationship exists (ie, orientation in the same axial plane) between lateral and medial surfaces, ie, superior frontal gyrus on the lateral surface of SFS is in the same plane as it is on the medial surface (Figure 2). The middle frontal gyrus is in the same plane as the cingulum on the medial SFS surface. The centrum semiovale is situated between the middle frontal gyrus and cingulum (Figure 3).

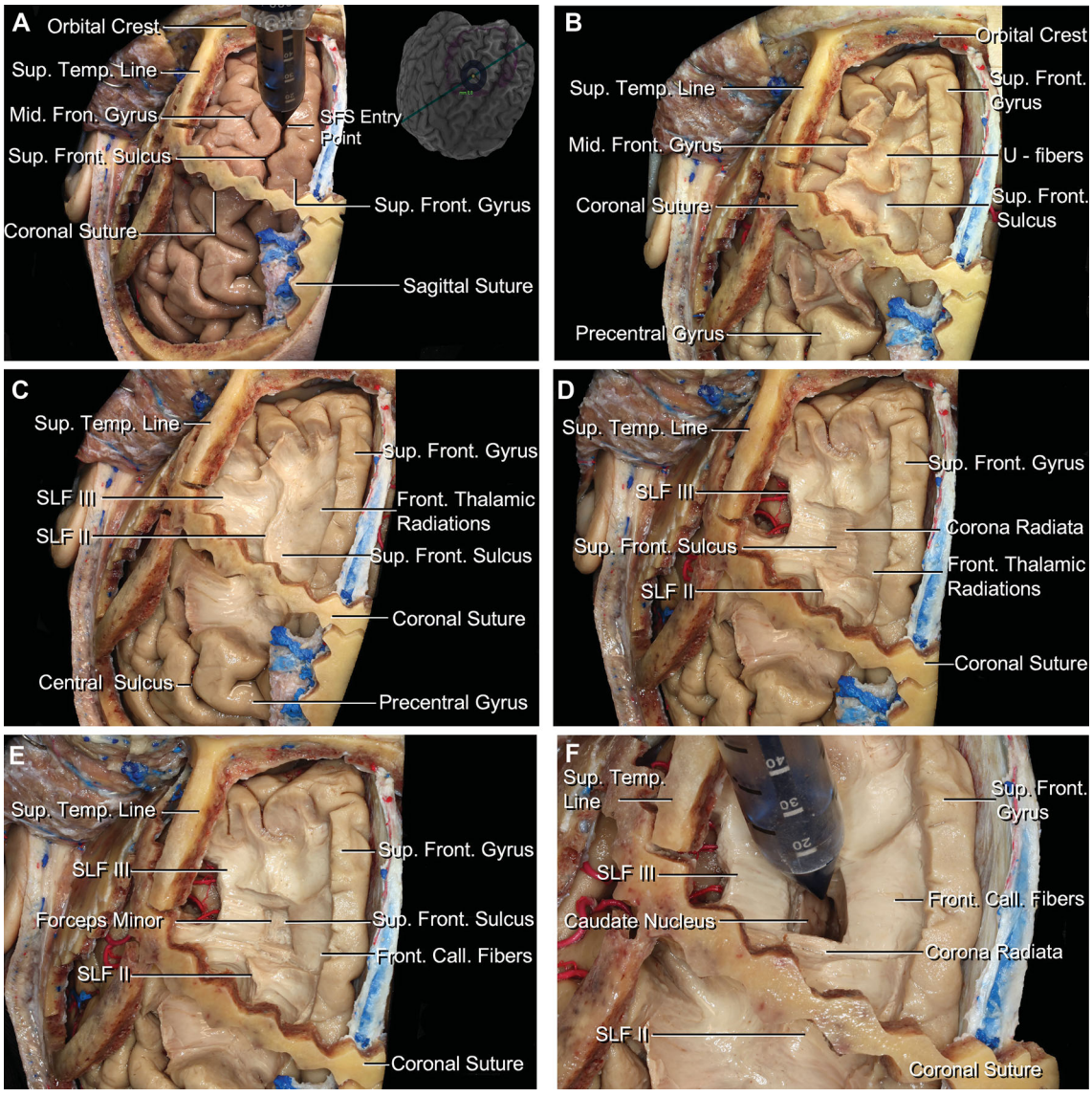

FIGURE 1. *An anatomical view of the anterior surgical corridor, layer by the layer using WMTs as a framework.* **A**, *OCRC: the BrainPath port device (NICO Corporation, Indianapolis, Indiana) is positioned along the middle division of the SFS (SFS). In addition, the relevant osseous landmarks are observed.* **B**, *OCRC. The divisions of the SFS. The anterior division extends from the PCS to the coronal suture. It is important to note here that the SFS begins at the PCS. The middle division extends 3.0 cm anterior to the coronal suture. The distal division corresponds to the end of the SFS in relation to the projection to the orbital crest. Following removal of the cortex, the first layer of the WMT in the SFS is formed by the U-fibers. The sulcal entry point is situated between the U-fibers formed by the superior and middle frontal gyri.* **C**, *The U-fibers were removed, and the parallel tracts of the corridor are now revealed. The medial fibers are formed by the corona radiata, frontal callosal fibers, and the superior longitudinal fascicle I (SLF-I), and the lateral fibers are formed by the SLF-II.* **D**, *The SLF-II lies: (a) lateral to the FAT in the proximal division of the SFS; (b) lateral to the IFOF and CCFs in the middle and distal divisions of the SFS; (c) superior and medial to SLF-III; and (d) in the same plane as CB (Figure 3A). SLF-II is located in all 3 divisions of the SFS. The SLF-II is removed, and the group of the fibers of the corona radiata is now revealed. The fibers now situated medial to the corridor are formed by the corona radiata, frontal callosal fibers, and the cingulum, and the lateral fibers continue to be formed by the SLF-II.* **E**, *The corona radiata is now removed, and the frontal callosal fibers are shown above the frontal horn. The fibers situated medially are now the frontal callosal fibers, and the lateral fibers are the SLF-III.* **F**, *The BrainPath port device is collocated in the SFS en route to the third ventricle. The corpus callosum was transected only to show a panoramic and anatomic view when the 0.9-mm atraumatic tip of the port crosses the frontal callosal fibers. Call: callosal; Front: frontal; Mid: middle; SLF: superior longitudinal fasciculus; Sup: superior; Temp: temporal. Front: frontal; Inf: inferior; Mid: middle; Precen: precentral; Sup: superior.*

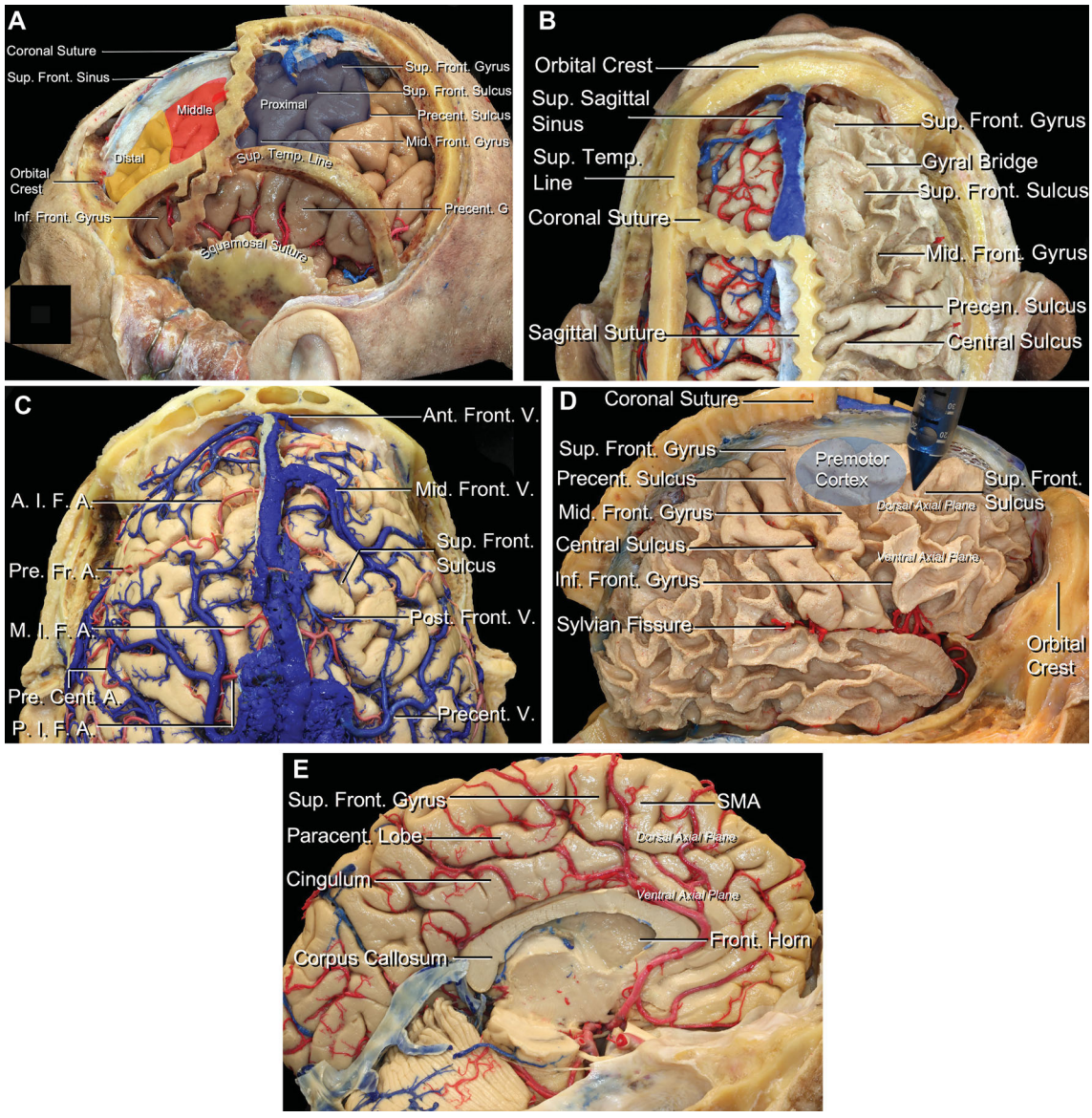

FIGURE 2. *Relevant anatomic landmarks of the outer ring (OCRC) and the inner ring (ICRC).* **A**, *Panoramic sagittal view of the proximal, middle, and distal divisions of the SFS (highlighted in green, red, and yellow, respectively). Explicitly, osseous (coronal suture, superior temporal line, and orbital crest) and gyral (superior, middle, and inferior frontal gyri) landmarks are shown.* **B**, *Axial ("bird's eye") view of venous and arterial structures in relation to the SFS. Explicitly, the arteries of the middle cerebral artery and the anterior cerebral artery are displayed with relation to the SFS on the left side. The veins along the SFS are shown on the right side.* **C**, *Similar axial view displaying the osseous landmarks, gyri, sulcus, and vessels are shown in relation to the SFS on the left. The gyri are removed on the right to highlight the sulcal orientations. The U-fibers of the SFS are shown in relation with the osseous landmarks.* **D**, *The SFS is now shown in relation to the precentral, superior, and middle frontal gyri. In addition, the BrainPath port device (NICO Corporation, Indianapolis, Indiana) can now be seen entering along the middle division of the SFS en route to the third ventricle. The relative position of the premotor cortex is highlighted in relation to the port trajectory.* **E**, *Medial surface of the brain. The WMTs are located medially and parallel to the surgical corridor in a superior to inferior orientation—SLF-I, cingulum, and corpus callosum. The SLF-I is located medial to the callosal fibers, above the cingulum and parallel to the surgical corridor of the SFS. The CB is situated superior to the CC, inferior to SLF-I, and lying in the same plane as the SLF-II and MFG. They are located medial to the corona radiata fibers and lateral to the SLF-I and cingulum. The relative orientation of the dorsal and ventral plane can be seen. A. I. F. A.: anterior internal frontal artery; Ant: anterior; Front: frontal; Mid: middle; Inf: inferior; M. I. F. A.: middle internal frontal artery; P. I. F. A.: posterior internal frontal artery; Precen: precentral; Pre. Cent. A.: precentral artery; Pre. Fr. A.: prefrontal artery; Post: posterior; Sup: superior; Supp: supplementary; Temp: temporal; V: vein; Vent: ventricle.*

TABLE 1. The Anatomic-Surgical Divisions of the SFS in Relation to the Outer and ICRCs

SFS – divisions	Osseous	OCRC Gyri	Vascular	ICRC WMT	Topographic correlation with the ventricular space Ventricle
Proximal	Sagittal, coronal suture, and superior temporal line	Posterior segment of the superior and middle frontal gyri Supplementary motor complex premotor cortex	Arteries precentral artery and PIFA veins: posterior frontal and precentral veins	SLF II FAT Frontal striatal tract Fronto pontine fibers Superior thalamic peduncle CCF Frontal callosal fibers SLF I Cingulum	Body of the lateral ventricle
Middle	Sagittal, coronal suture, and superior temporal line	Middle segment of the superior and middle frontal gyri	Arteries: Precentral artery and MIFA vein: middle frontal vein	SLF II IFOF Anterior thalamic peduncle Fronto striatal tract Fronto pontine tract CCF Frontal callosal SLF I Cingulum	Frontal horn. Third ventricle (anterior and middle part)
Distal	Frontal bone orbital crest and superior temporal line	Anterior segment of the superior and middle frontal gyri	Arteries: prefrontal artery and AIFA vein: anterior frontal vein	Anterior thalamic peduncle Fronto striatal tract Frontopontine tract CCF Forceps minor Cingulum	Frontal horn and third ventricle (middle part)

OCRC = Outer Circumferential Radial Corridor, ICRC = Inner Circumferential Radial Corridor, PIFA = Posterior Internal Frontal Artery, MIFA = Middle Internal Frontal Artery, SLF II = Superior Longitudinal Fasciculus II, SLF I = Superior Longitudinal Fasciculus I, IFOF = Inferofrontal occipital fasciculus.

TABLE 2. Relevant WMTs of the SFS Corridor

Division – SFS	Medial of the SFS	Intervening of the SFS	Lateral of the SFS
Proximal	SLF I FAT Cingulum Frontal callosal fibers	Corona radiata FAT CCF	SLF II IFOF SLF III CCF
Middle	SLF I FAT Cingulum Frontal callosal fibers	Corona radiata FAT CCF	SLF II IFOF SLF III CCF
Distal	Forceps minor Cingulum	Corona radiata	IFOF CCF

SLF I = superior longitudinal fasciculus I; SLF II = superior longitudinal fasciculus II; FAT = frontal aslant tract; IFOF = inferior fronto-occipital fasciculus; CCF = claustrocortical fiber; SLF III = superior longitudinal fasciculus III.

The Inner Ring

Inner circumferential-radial corridor: the principle constituent of ICRC are WMTs (Table 2). Following decortication of superior frontal gyrus and middle frontal gyrus, the underlying WMTs of SFS complex were exposed. The subcortical network of SFS was then divided into 3 segments based on the SFS meridian (a vertical extension of SFS to the skull base):

i) SFS-medial segment medial to SFS meridian;
ii) SFS-lateral segment lateral to SFS meridian; and
iii) Intervening segment directly underlying SFS (Figure 3 and Table 3).

Medial Segment

Frontal aslant tract (FAT): FAT travels obliquely from medial to lateral in a coronal/lateral plane, connecting the pars opercularis of the inferior frontal gyrus to the supplementary motor area (SMA) and pre-SMA. Fibers reach the pars triangularis and the inferior region of the precentral gyrus. FAT is located medially in relation to SLF-II and laterally in relation to claustrocortical fibers (CCF). In the sagittal/anterior-posterior plane, imperatively, FAT extends 1.96 cm anterior to coronal suture reaching into SMA (Figure 4 and Table 4).

Cingulum bundle: It originates from the temporal pole and circumferentially wraps around corpus callosum before terminating anteriorly and inferiorly at the genu of the corpus callosum,

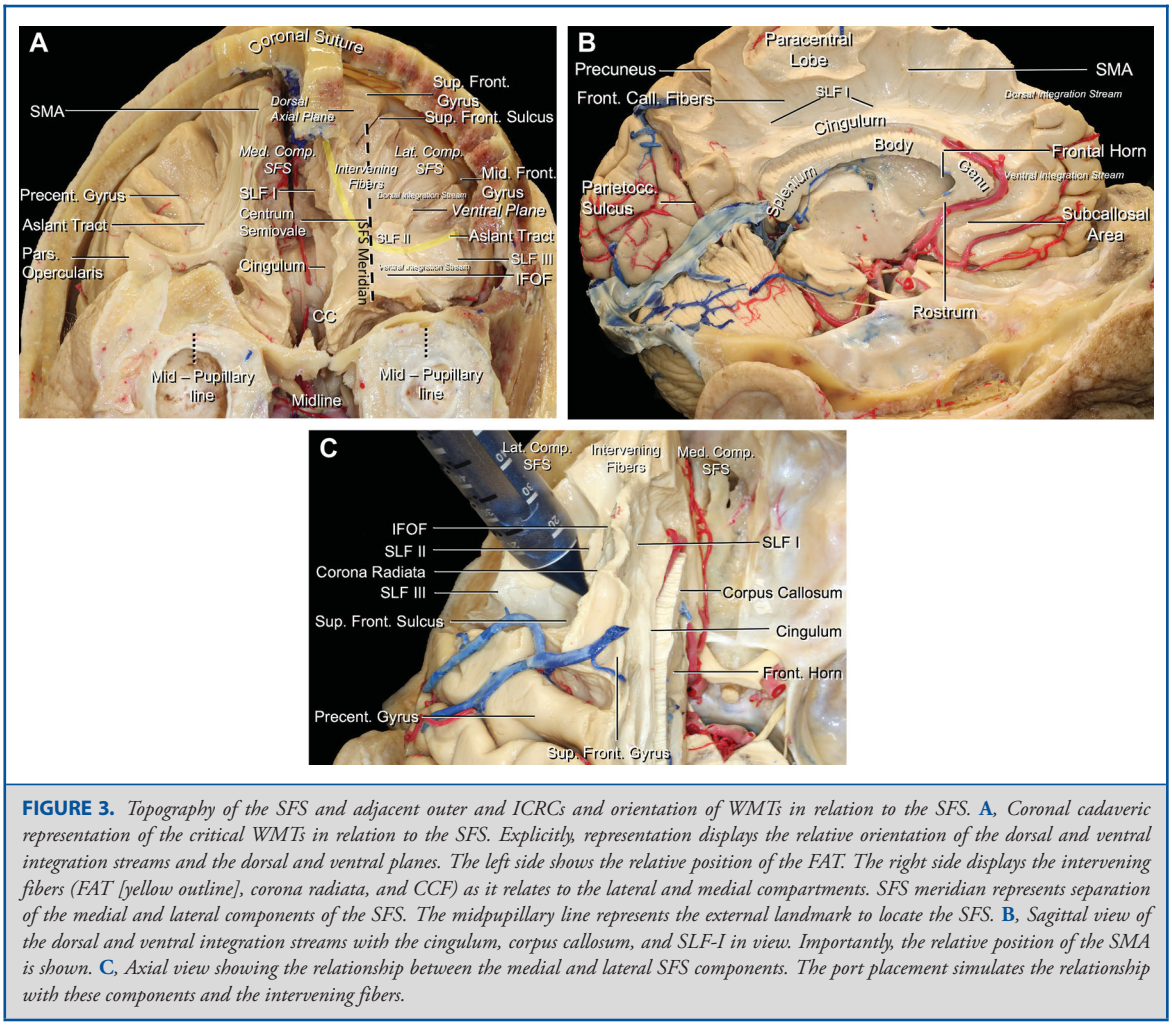

FIGURE 3. *Topography of the SFS and adjacent outer and ICRCs and orientation of WMTs in relation to the SFS.* **A**, *Coronal cadaveric representation of the critical WMTs in relation to the SFS. Explicitly, representation displays the relative orientation of the dorsal and ventral integration streams and the dorsal and ventral planes. The left side shows the relative position of the FAT. The right side displays the intervening fibers (FAT [yellow outline], corona radiata, and CCF) as it relates to the lateral and medial compartments. SFS meridian represents separation of the medial and lateral components of the SFS. The midpupillary line represents the external landmark to locate the SFS.* **B**, *Sagittal view of the dorsal and ventral integration streams with the cingulum, corpus callosum, and SLF-I in view. Importantly, the relative position of the SMA is shown.* **C**, *Axial view showing the relationship between the medial and lateral SFS components. The port placement simulates the relationship with these components and the intervening fibers.*

with projections to the superior frontal gyrus (Figures 3, 4 and Table 2, 3 and 4).

Superior longitudinal fasciculus I (SLF-I): SLF is divided into 3 segments organized as an ascending stairwell from inferior-lateral to superior-medial: (1) SLF-III situated under inferior frontal gyrus extends to supramarginal gyrus, (2) SLF-II (described below), and (3) SLF-I under superior frontal gyrus. SLF-I, an association fiber, extends from precuneus to superior frontal gyrus terminating in SMA and premotor areas of the frontal lobe (Figures 3, 4 and Table 2, 3 and 4).

Lateral Segment

U-fibers: Short association fibers connecting superior and middle gyri.

SLF II (SLF-II): SLF-II, an association fiber, runs parallel to SFS, extending from angular gyrus to middle frontal gyrus at level of the body of the lateral ventricle and corpus callosum (Figure 1, 2, 3, and 4).

Inferior fronto-occipital fasciculus (IFOF): IFOF is a long association tract, running from the anterior and middle part of the middle frontal gyrus and inferior frontal gyrus to the posterior portion of the parietal and occipital lobes (optic radiations) (Figure 2).

To avoid confusion, note, SFS topography is divided into divisions (AP-axis) and WMTs below SFS are compartmentalized into segments (Rostral-caudal axis), ie, medial segment refers to the WMTs organization juxtaposed beneath the SFS, whereas the middle division refers to the topography of SFS representing the division between the SFS-PD and SFS-DD (Figure 2 and 3).

Intervening Segment

Of note, FAT and CCF represent true crossing fibers that begin in the medial segment and traverse across the intervening segment into the lateral segment terminating in the IFG and operculum (Figures 3, 4 and Tables 2, 3).

Corona radiata: These group of fibers are a vital projection system, run within the intervening region and the ventricle

TABLE 3. WMTs of the SFS Complex: Connectivity and Functional Role

	Cortical connectivity	Dominant hemisphere	Nondominant hemisphere
Lateral SFS Segments			
U-fibers	SFG-MFG	Short association fibers connecting gyri at any point in cerebral cortex	Short association fibers connecting gyri at any point in cerebral cortex
SLF II	Angular gyrus – midpart of the middle frontal gyrus	Visual and oculomotor aspects of spatial function spatial working memory attention	
Inferofrontooccipital fasciculus	Frontal pole, Orbito-fronto cortex, IFG, MFG and SFG – Planum temporal, SPL and occipital cortex	Lexical-semantic processing, visual spatial processing Reading, attention, and visual processing	Lexical-semantic processing
Corona radiata – intervening segment			
CCF *(crossing fiber)*	Claustrum to orbitofrontal areas Premotor area SMA	Executive function, cognitive control Executive function, cognitive control Sensory guidance of movement	Executive function, cognitive control Executive function, cognitive control Sensory guidance of movement
Thalamic prefrontal peduncle	Anterior, medial, the ventral posterior part of the medial, lateral dorsal and lateral posterior nuclei to areas in the prefrontal cortex included the SFG, MSFG, MFG, Ptri, Porp, LOG, and AOG.	The function of the prefrontal cortex has been researched extensively and includes cognitive abilities, social emotion, executive functioning, motor control, and language	The function of the prefrontal cortex has been researched extensively and includes cognitive abilities, social emotion, executive functioning, motor control
Frontopontine fibers	Premotor, prefrontal, and dorsolateral prefrontal cortex (SFG and MFG) to the pontine nuclei	Motor function and connection to the cerebellum	Motor function and connection to the cerebellum
Frontal striatal tract	Pre-SMA and SMA proper to the anterior part of the caudate nucleus and putamen	Verbal fluency in speech; voluntary motor control	Voluntary motor control
Corticospinal tract corticobulbar tract	Motor area, premotor, supplementary area, motor cortex of the cingulum and the postcentral gyrus to the spinal cord.	Pyramidal motor system	Pyramidal motor system
Medial SFS segments			
FAT *(crossing fiber)*	Pre-SMA and SMA proper – pars opercularis and pars triangularis		Speech initiation verbal fluency
Callosal fibers	Superior frontal gyrus – superior frontal gyrus Frontal callosal	Motor, sensory, and cognitive integration between cerebral hemispheres	Motor, sensory, and cognitive integration between cerebral hemispheres
Cingulum bundle	Temporal pole – rostral subcallosal area in the orbital frontal cortex	Executive function, decision-making, and emotion processing Execution of motor- and attention-related tasks Cognitive function.	Executive function, decision-making, and emotion processing Execution of motor- and attention-related tasks Cognitive function
SLF I	Precuneus – pre-SMA and SMA proper	Regulation of higher aspects of motor function, initiation of motor activity, activation in resting state, integration of internally and externally driven information	Regulation of higher aspects of motor function, initiation of motor activity, activation in resting state, integration of internally and externally driven information

SFG = superior frontal gyrus, IFG = inferior frontal gyrus, MFG = middle frontal gyrus, SPL = superior parietal lobule, MSFG = medial superior frontal gyrus, Ptri = pars triangularis, Porp = pars opercularis, AOG = anterior orbital gyrus, LOG = lateral orbital gyrus, SMA = supplementary motor area.

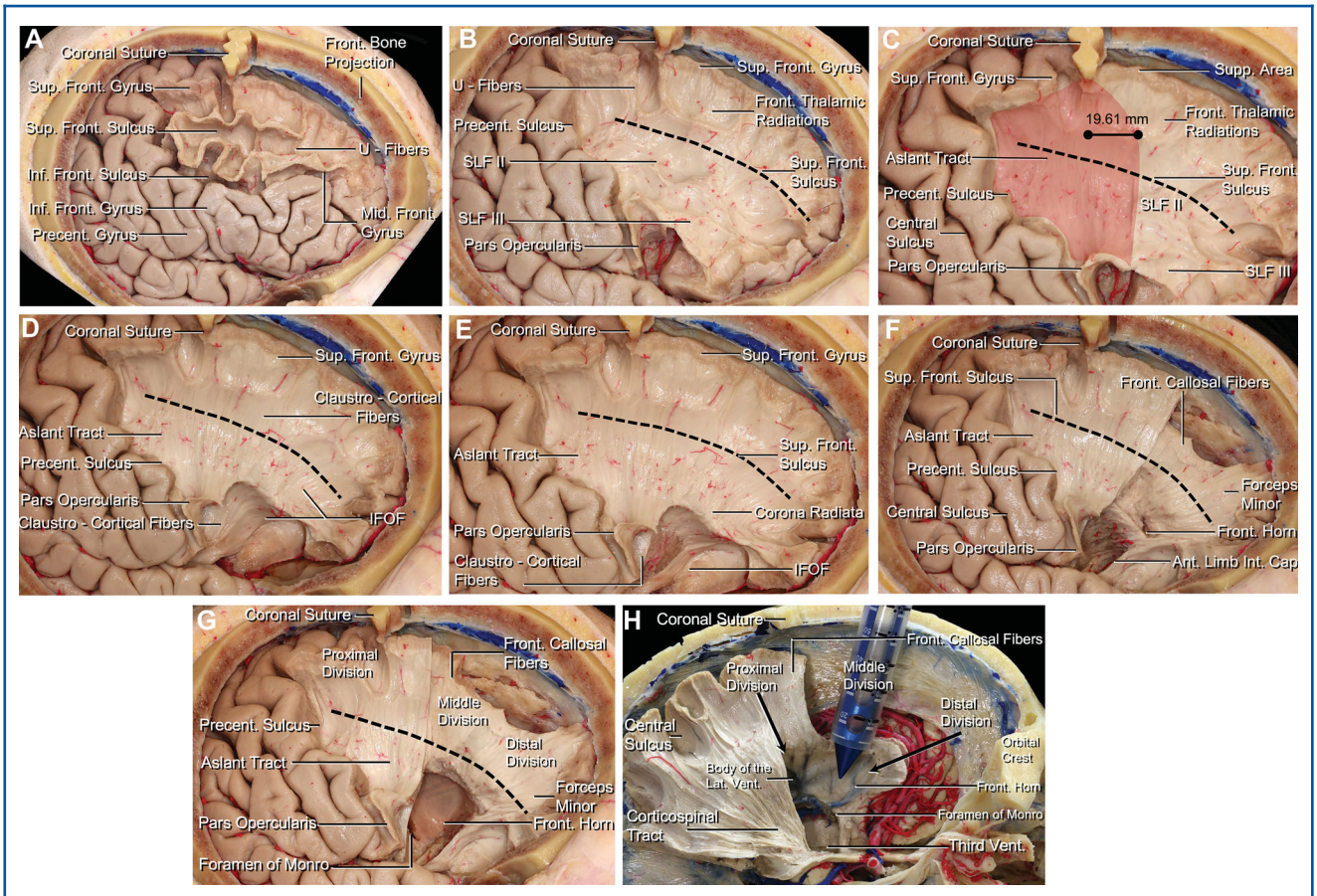

FIGURE 4. *Sagittal exposure of the relevant WMTs in relation to the divisions of the SFS.* **A** *and* **B**, *The U-fibers were removed in the superior frontal and middle frontal gyri to reveal the frontal thalamic radiations and SLF-II, respectively. The SLF-II located in the anterior part of the SFS and was removed to reveal the FAT.* **C**, *The edge of the FAT is situated 1.96 cm anterior to the CS. The SLF-II and aslant tract are observed in the middle division of the SFS.* **D**, *The aslant tract is preserved in the anterior and middle division. The IFOF is situated lateral to the CCF of the external capsule and medial to the SLF-II. The CCF lie medial to the FAT and the SLF-II and lateral to the fibers of the internal capsule. The SLF-II was removed to reveal the CCF and the IFOF.* **E**, *FAT is preserved, and the CCF and IFOF were removed to reveal the fibers of the corona radiata, which is present in all 3 divisions of the SFS.* **F**, *After the removal the fibers of the corona radiate, the callosal fibers are now revealed.* **G**, *The frontal callosal fibers and the forceps minor are now observed in relation to the frontal horn and respectively with the middle and distal division of the SFS.* **H**, *The projection of the ventricle with the divisions of the SFS is shown. The port is placed along the distal division of the SFS toward the frontal horn of the lateral ventricle. Ant: anterior; Front: frontal; Inf: inferior; Int; internal; IFOF: inferior fronto-occipital fasciculus; Lat: lateral; Mid: middle; Precen: precentral; SLF: superior longitudinal fasciculus; Sup: superior; Temp: temporal; Vent: ventricle.*

medially, under SFS along its vertical long axis, lending themselves to parafascicular approaches.

Subnetworks of corona radiata:

I. CCF are projection fibers extending from the claustrum that branch out to the dorsal external capsule and intermingle with fibers of corona radiata.
II. Superior thalamic peduncle are tracts that represent a group of projection fibers running vertically from the premotor cortex, precentral, and postcentral gyrus to the thalamus and vice versa.
III. Anterior thalamic peduncle is formed by projection fibers, interplay between dorsolateral prefrontal cortex, orbitofrontal region, cingulate gyrus, and anterior and midline nuclear group of the thalamus. The fibers run obliquely and horizontally.
IV. Frontopontine fibers are projection fibers from the superior and middle frontal gyri and course through the anterior limb of the internal capsule to the inner-third of the base of the cerebral peduncles terminating in pontine nuclei.
V. Frontal striatal tract connects premotor cortex with putamen and the caudate nuclei, prefrontal cortex with caudate nucleus, and pre-SMA with caudate nucleus.
VI. Corticospinal tract courses within the posterior limb of the internal capsule to terminate at the middle third of the cerebral peduncle; imperatively, a portion of this is formed by

TABLE 4. Measurements of the FAT and SLF II

Hemispheres	FAT CS-Ant to CS	SSS-SLF II
1	1.98 cm	2.97 cm
2	1.93 cm	2.95 cm
3	1.93 cm	3.1 cm
5	1.99 cm	2.9 cm
6	1.96 cm	3.1 cm
7	1.98 cm	2.95 cm
8	1.94 cm	3.12 cm
9	1.97 cm	3.06 cm
10	1.95 cm	2.9 cm
Average	1.96 cm	3 cm
SD	0.02	0.08

fibers of the SMA, perhaps, providing an anatomic substrate for "SMA-Syndrome."

Callosal fibers: These fibers are formed by frontal callosal fibers and forceps minor. The frontal callosal fibers, formed by fibers originating from superior and middle frontal gyri, connect to the mirrored gyri of the contralateral hemisphere via the body of the corpus callosum. This covers the posterior portion of the frontal horn and the anterior portion of the body of the lateral ventricle. The forceps minor are fibers crossing the genu connecting both prefrontal and orbitofrontal regions covering the anterior part of the frontal horn.

Figure 5 represents a 3D artistic rendering of the outer and inner rings of the SFS corridor, displaying the relative positions and segments of key osseous, cortical (sulci and gyri), vascular, and WMT structures.

Table 3 describes WMTs of the SFS complex with a brief description of cortical connectivity and theoretical function given the sparsity of data demonstrating clearly defined neurocognitive function of specific WMTs bilaterally. Although not the primary intent of this report, we reviewed the available literature and have provided a summary of the presumed functional importance of WMTs juxtaposed in the SFS subcortical region. This is only intended to provide the reader with a convenient overview based on data previously described and a template for additional evolving functional knowledge.

Diffusion-Tensor Imaging Correlation

TPCS through KM-EP was simulated in diffusion-tensor imaging (DTI)-tractography models. All relevant tracts relative to SFS were successfully modelled; with the exception of the tracts of the corona radiata, only the corticospinal tract could be separately segmented given the inherent limitations of current-state software to detect crossing fibers (Figure 6).

Clinical Case Examples

Two clinical cases are presented: (a) colloid cyst demonstrating applicability for a commonly encountered pathology (**Video**, **Supplemental Digital Content**), and (b) large central neurocytoma illustrating feasibility of a large vascular lesion resected

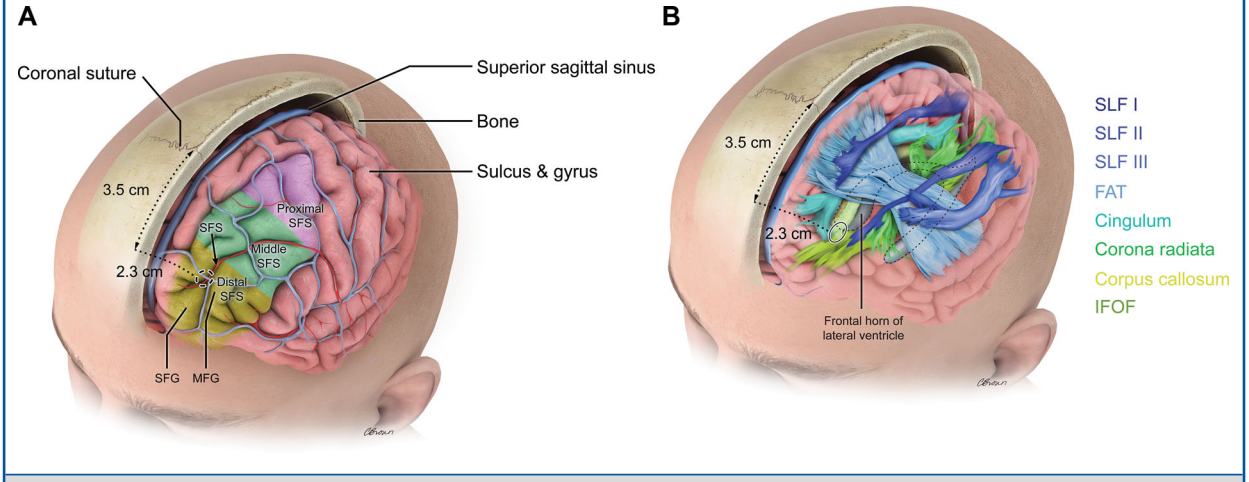

FIGURE 5. *Artistic 3D illustration of the SFS corridor.* **A**, *Outer ring: the coronal suture represents the key osseous fiduciary landmark that separates the SFS into 2 of its 3 segments—the proximal and middle divisions. The SFS complex is divided into 3 divisions: (1) proximal (in purple) extends from precentral sulcus to coronal suture; (2) middle (in green) extends 3.0 cm anterior to coronal suture; and (3) distal (in yellow) extends from the distal end of middle division to the orbital crest. The coordinates of the SFS Parafascicular EP (dotted circle) are 3.5 cm anterior to coronal suture and 2.3 cm lateral to the midline or SSS.* **B**, *Inner ring: the relative position and orientation of the relevant WMTs are shown: SLF-I, II, and III (dark blue), FAT (light blue), cingulum (turquoise), corona radiata (green), corpus callosum (yellow), and IFOF (light green). The SFS parafascicular entry point is shown here (black circle, x = 2.3, y = 3.5, and z = parallel to corona radiata) traversing between cingulum and SLF-II, en route to the frontal horn of the lateral ventricle. Artistic illustration © Cora Brown, 2019. Used with permission.*

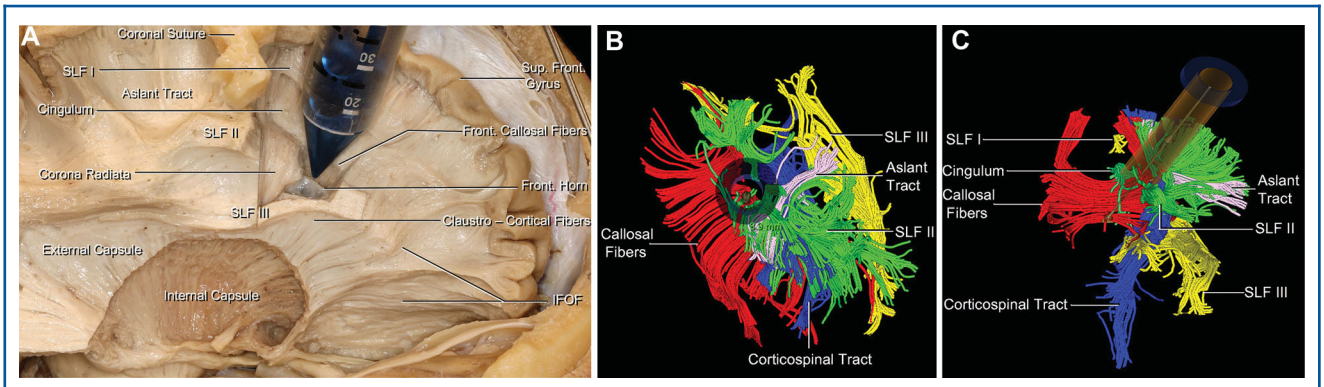

FIGURE 6. *SFS parafascicular EP. The SFS parafascicular EP, which is 3.5 cm anterior to the CS and 2.3 cm lateral, avoids SLF-II and FAT because of its relatively anterior trajectory (x = 2.3, y = 3.5).* **A**, *Sagittal cadaveric model displaying the relative position of the port trajectory in relation to the relevant WMTs fibers. Explicitly, the trajectory is placed in the distal division of the SFS and angled parafascicular to the corona radiata and parallel to the long axis of the internal capsule. In addition, port placement is placed at the frontal horn of the lateral ventricle, traversing only the frontal callosal fibers (opening diameter = 0.9 mm), and is medial to the FAT, lateral to the CCF, SLF III and IFOF, and anterior to SLF-II.* **B** *and* **C** *represent radiological correlates with simulated down-the-barrel and oblique views, respectively, with the relative position and orientation of relevant WMTs fibers. Front: frontal; IFOF: inferior fronto-occipital fasciculus; SLF: superior longitudinal fasciculus; Sup: superior.*

via TPCS through the proposed SFS corridor. Pre-, intra-, and postoperative information are described in detail in Table 5; pre and postoperative DTI imaging demonstrates the surgical footprint (Figure 7). The **Video**, **Supplemental Digital Content** describes the surgical case of the colloid cyst resection, including a preoperative planning schema using 3D modelling and tractography, anatomic nuances of the surgical corridor, and surgical technique.

DISCUSSION

Traditional surgical approaches to the frontal subcortical region, frontal horn, and third ventricle often require traversing cortical and subcortical structures.[2-4,15,24,25] We report a transsulcal alternative founded on an anatomically based surgical paradigm governed by WMTs underlying the SFS corridor. We propose a pragmatic surgical system based on 2 axes: (a) anterior-posterior axis; SFS divisions designed to mitigate anatomic risk to key projection fibers: FAT, by entering distally to it, and corona radiata, by paralleling it; and (b) Rostral-Caudal axis; WMT-framework underlying the SFS, based on the SFS meridian (medial, lateral, and intervening segments), designed to minimize risk to key association fibers (SLF-II/cingulum [medially] and SLF-III/IFOF [laterally]) (Table 6).

The intent of this report is to detail the anatomic underpinnings of our schema in order to facilitate individualized corridors to the subcortical frontal lobe, ventricular, and juxta-ventricular region.

SFS Morphological Variability

The morphology and dimensions of the SFS can be variable; Ono et al[19] described shallow sulci located in superior frontal gyrus connecting to SFS, which they referred to as medial frontal sulci or superior frontal paramidline sulci. Ribas et al[26] described SFS as being interrupted in 50% of specimens. The length of its continuous proximal division adjacent to the precentral sulcus was 5.74 cm. Koutsarnakis et al[27] noted SFS was continuous in 12 and interrupted in 8 hemispheres. They reported a mean length and depth of 6.7 cm and 1.7 cm, respectively. Notably, we have found SFS was interrupted in 3/5 (60%) of specimens most prominently in SFS-PD and SFS-MD.

Anatomic Classification

Given this variability, and in order to better conceptualize an anatomically based reproducible corridor, we divided the SFS corridor into 2-layered circumferential rings sequentially encountered as the surgeon travels from the surface to the depths radially towards the ventricles. The KM-EP to the ventricle engages a specific division of SFS mitigating the anatomic risk of subcortical injury. Two points (entry point and target) create a trajectory; the angle of which is adjusted, by manipulating either point, to be parafascicular to corona radiata. Given that the TPCS, when using a port, only requires engaging a limited portion of the SFS; specifically, 13.5 mm in inner diameter (15.5 mm outer diameter), discontinuity is not a barrier if the specific division can be consistently identified; therefore, SFS-PD and SFS-MD are not ideal.

Proximal Division

Few studies have described the transsulcal approach through the SFS. Ribas et al[26] described posterior coronal point, the intersection of the precentral sulcus with the SFS, located 1 cm posterior to coronal suture and 3 cm lateral to SSS. It should be noted that Ribas's[26] "posterior" point is an anatomic reference, and in our schema, this entry point (EP) would engage

TABLE 5. Clinical Case Examples Describing the Utilization of the SFS Corridor

Clinical Case	Age	Gender	Pathology	Tumor size (cm^2)	Image findings	Preoperative neurological deficits	SFS entry segment	Trajectory	IntraOp changes	PostOp neurological recovery
1	22	F	Colloid cyst	0.7	Homogenously enhancing mass at the roof the third ventricle at the level of the FM	-Headache-Nausea-Vomiting-Phonemic verbal fluency-Visuospatial-Learning and memory-Executive functioning	Distal	Frontal horn of Left LV Towards FM	No changes in neurocognitive, sensorimotor, and speech	Full recovery in all neurocognitive domains
2	21	F	Central neurocytoma	4.6	Multiloculated vascular mass in left lateral ventricle extending into FM	-Headache-Diplopia-LE paresthesia-Photophobia-Phonophobia-Verbal fluency and recall	Distal	Frontal horn of left LV	Improvement in short-term memory recall (1 to 2 words)	Improvement in short-term memory only-Remaining domains returned to baseline

SFS-PD, directly placing FAT at risk. Based on the circuitry, the risk of speech fluency, apraxia, and SMA syndromes is anatomically significant using this corridor. Given these risks, we recommend utilizing the SFS-PD with caution, and preferably under awake conditions, to access pathologies of the subcortical region. In fact, in our practice, we reserve this for rare relatively superficial posterior subcortical regions; rarely if ever, would we consider this corridor for ventricular access.

Utilization of the SFS to the anterior ventricular system, as described by Koutsarnakis et al,[27] focused on specific WMT fibers along limited sulcal segments, namely, intervening segment, based on our classification. However, the medial and lateral segments were not considered, creating potential risk to fibers such as SLF-II and cingulum. Additionally, their exposure requires microsurgical dissection of the entire SFS using retractors. Consequently, this dissection (approximately length and depth of 6 and 2 cm, respectively) poses a risk to cortical and subcortical structures.[28-31]

Middle Division

In order to preserve FAT in the sagittal/anterior-posterior (y-axis), the surgical approach should be at least 1.96 cm anterior to coronal suture (Figure 2, 3 and 4). Same considerations, as discussed above, with respect to limited access to subcortical lesions and ventricular lesions, apply to the middle division.

Distal Division

Given the relatively small, 1.4-cm, window available in the middle division, which approximates the 13.5-mm inner diameter (15.5-mm outer diameter) of the port we use, we sought to identify a more forgiving window to enter the SFS and create parafascicular trajectories. We have developed and clinically applied a specific EP along the distal division of the SFS, the KM-EP($x = 2.3$ cm, $y \geq 3.5$ cm), which engages the SFS at a minimum of 3.5 cm (y-axis/AP) anterior to coronal suture, representing a region devoid of FAT. The details of this EP in comparison to historical access points are beyond the scope of this report and are reported separately. In the coronal/lateral plane (x-axis), SFS is noted to be 2.3 cm lateral from SSS to avoid SLF-II. In addition, we also use this point for ventricular cannulation (drains/shunts) rather than Kocher's point. A direct anatomical comparison of ventricular entry points, currently used in clinical practice and reported in the literature, is the subject of an accompanying report.

Limitations

A clear limitation of cadaveric models is the required stepwise dissections to illustrate the respective trajectories that result in disruption of superficial WMTs in order to visualize the deeper underlying fibers, therefore creating the appearance of transection of these fibers. In addition, it is important to note that there may lie an inherent operator variability in fiber dissection technique when attempting to precisely segmenting and identifying white matter fiber bundles. This can be due to a variety of factors,

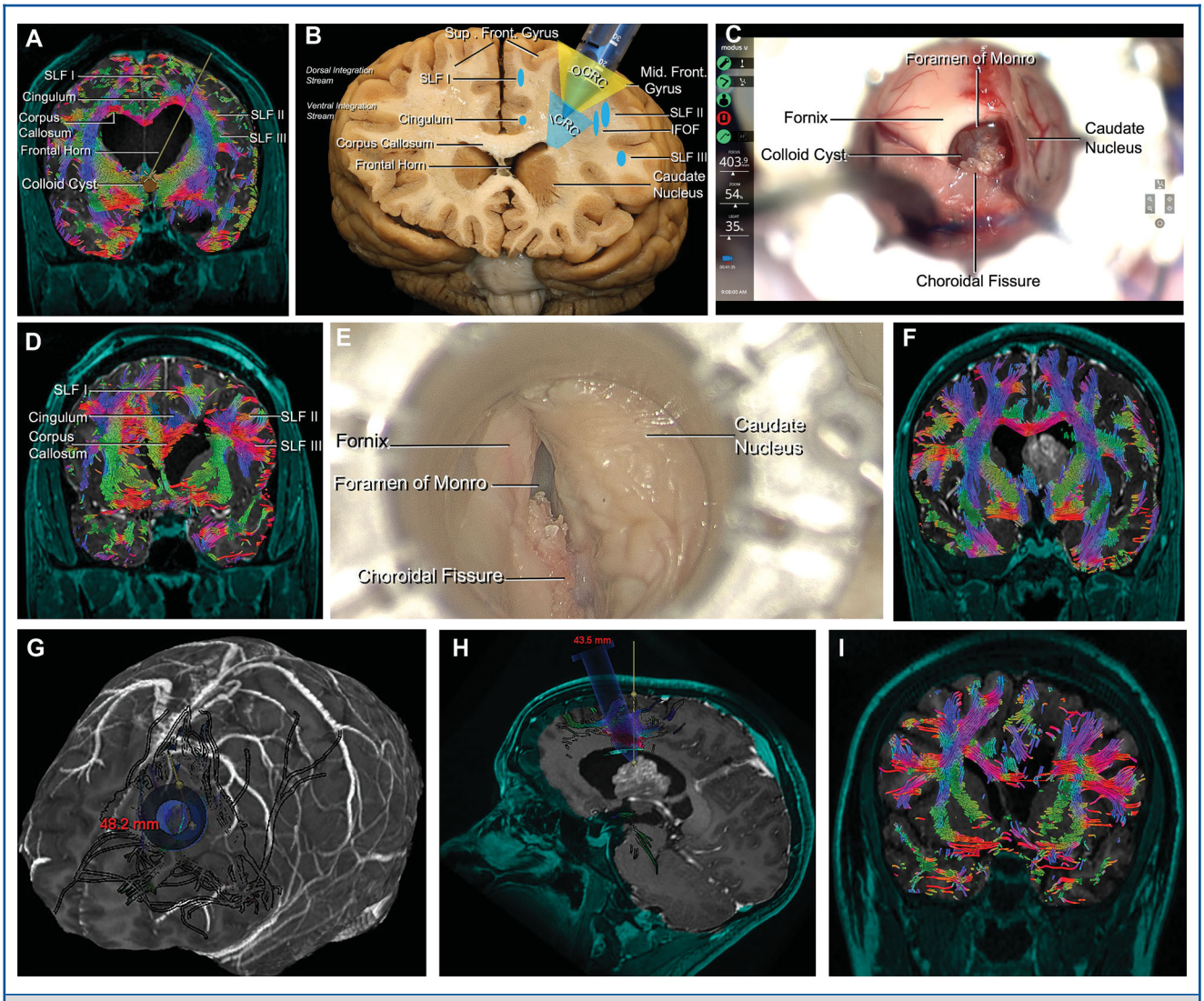

FIGURE 7. ***Video*, *Supplemental Digital Content****: surgical case examples. Colloid cyst.* **A**, *Preoperative planning with MRI-Tractography of the transsulcal-parafascicular corridor and* **B**, *coronal anatomical view of the same intraoperative view as in* **A**. *The port is collocated in the SFS and addressed to the frontal horn with the relative OCRC and ICRC compartment highlighted. In addition, the parallel tracts are observed in relation to the port.* **C**, *Intraventricular surgical view with exoscopic visualization system was used to visualize the frontal horn and the foramen of Monro, namely the robotically operated video optical telescopic microscope (ROVOT-m).* **D**, *Postoperative tractography revealing complete resection of the cyst. The parallel tracts are preserved, and the fibers of the corona radiata can be seen separated with only the frontal callosal fibers transected.* **E**, *Anatomical intraventricular view simulated with ROVOT-m is correlated with* **C**. *Central Neurocytoma.* **F**, *Preoperative MR-DTI imaging revealing a large multiloculated mass in the left lateral ventricle extending into the foramen of Monro.* **G**, *Preoperative brain model planning showing relative trajectory of the port in relation to cortical vessels, sulci, and WMTs.* **H**, *Sagittal preoperative planning MR-DTI imaging showing trajectory towards the lateral ventricle and foramen of Monro.* **I**, *Postoperative MR-DTI revealing minimal surgical footprint and GTR. Both cases were performed under awake anesthesia and utilized the BrainPath port system for SFS sulcal entry and resection. IFOF: inferior fronto-occipital fasciculus; SLF-I: superior longitudinal fasciculus I; SLF-II: superior longitudinal fasciculus II; superior longitudinal fasciculus.*

including operator experience and ability, a priori anatomical knowledge, and, possibly more importantly, the inherent relative position and orientation of WHTs relative to each other (ie "kissing" fibers). For example, accurate delineation of fine fibers such as FAT, SLF-I, and SLF-II and noting their relative position, measurements, and osseous and vascular relationships may be difficult and limited in certain specimens but can be performed with careful and systematic dissection. In addition, IFOF can,

TABLE 6. Abbreviation Score Card

Keywords	Abbreviation
White matter tracts	WMT
Transsulcal parafascicular corridor surgery	TPCS
Magnetic resonance imaging	MRI
Diffusion-tensor imaging	DTI
Superior frontal sulcus	SFS
Outer circumferential-radial corridor	OCRC
Inner circumferential-radial corridor	ICRC
Frontal aslant tract	FAT
Supplementary motor area	SMA
Superior longitudinal fasciculus	SLF
Inferior fronto-occipital fasciculus	IFOF
Superior sagittal sinus	SSS
SFS proximal division	SFS-PD
SFS middle division	SFS-MD
SFS distal division	SFS-DD
SFS parafascicular entry point	SFSP-EP

in some cases, merge with CCF or fibers of the external and internal capsule; this may limit the ability to clearly delineate all fibers of the IFOF. With respect to the DTI-rendered images, there is variability with regards to voxel seeding, acquisition resolution, and degree of filtration of intersecting or "kissing fibers." Additionally, the clinical value of anatomic preservation remains to be systematically established. It is important for the reader to be clearly aware of these significant limitations in interpreting any of the results, data, and recommendations contained within this report.

CONCLUSION

The SFS represents an ideal corridor to access the subcortical frontal lobe, ventricle, and juxta-ventricular region. With the intent of minimizing the surgical footprint required, we have introduced a schema dividing the key subcortical WMT-framework surrounding the SFS into medial, intervening, and lateral segments, creating a reproducible customized anatomic corridor to optimize the preservation of the WMTs. Osseous landmarks serve as fiducials and thereby anatomically define a frontal transsulcal-parafascicular SFS module. Clinical studies will be needed to demonstrate the value of preserving these anatomic structures.

Disclosures

This work was supported by donations from NICO Corporation, Carl ZEISS United States, Stryker Corporation, and KARL STROZ Industrial-America, Inc. This research is also supported by an award to the Aurora Research Institute by the Vince Lombardi Cancer Foundation. Dr Kassam reports involvement as a consultant to Synaptive Medical, KLS Martin Medical, Consultant Stryker Corporation, and the Medtronic Advisory Board and as a founder and CEO of Neeka Health LLC.

REFERENCES

1. Yaşargil MG, Cravens GF, Roth P. Surgical approaches to "inaccessible" brain tumors. *Clin Neurosurg*. 1988;34:42-110.
2. Yasargil MG. A legacy of microneurosurgery: memoirs, lessons, and axioms. [Miscellaneous Article]. *Neurosurgery*. 1999;45(5):1025-1092.
3. Yasargil MG. Surgical concerns. In: *Microneurosurgery*. 3B. New York: Thieme; 1988:25-53.
4. Kelly PJ, Goerss SJ, Kall BA. The stereotaxic retractor in computer-assisted stereotaxic microsurgery. *J Neurosurg*. 1988;69(2):301-306.
5. Bander ED, Jones SH, Kovanlikaya I, Schwartz TH. Utility of tubular retractors to minimize surgical brain injury in the removal of deep intraparenchymal lesions: a quantitative analysis of FLAIR hyperintensity and apparent diffusion coefficient maps. *JNS*. 2016;124(4):1053-1060.
6. Jennings JE, Kassam AB, Fukui MB, et al. The surgical white matter chassis: a practical 3-dimensional atlas for planning subcortical surgical trajectories. *Oper Neurosurg*. 2018;14(5):469-482.
7. Monroy-Sosa A, Jennings J, Chakravarthi S, et al. Microsurgical anatomy of the vertical rami of the superior longitudinal fasciculus: an intraparietal sulcus dissection study. *Oper Neurosurg*. 2018;16(2):226-238.
8. Ritsma B, Kassam A, Dowlatshahi D, et al. Minimally invasive subcortical parafascicular transsulcal access for clot evacuation (mi space) for intracerebral hemorrhage, minimally invasive subcortical parafascicular transsulcal access for clot evacuation (mi space) for intracerebral hemorrhage. *Case Rep Neurol Med Case Rep Neurol Med*. 2014;2014(2014):e102307.
9. Eliyas JK, Glynn R, Kulwin CG, et al. Minimally invasive transsulcal resection of intraventricular and periventricular lesions through a tubular retractor system: multicentric experience and results. *World Neurosurg*. 2016;90:556-564.
10. Day JD. Transsulcal parafascicular surgery using brain pathâ® for subcortical lesions. *Neurosurgery*. 2017;64(CN_suppl_1):151-156.
11. Labib MA, Shah M, Kassam AB, et al. The safety and feasibility of image-guided brainpath-mediated transsulcul hematoma evacuation: a multicenter study. *Neurosurgery*. 2017;80(4):515-524.
12. Friedman MA, Meyers CA, Sawaya R. Neuropsychological effects of third ventricle tumor surgery. *Neurosurgery*. 2008;62(6 Suppl 3):1093-1100.
13. Eichberg DG, Buttrick SS, Sharaf JM, et al. Use of tubular retractor for resection of colloid cysts: single surgeon experience and review of the literature. *Oper Neurosurg*. 2018;16(5):571-579.
14. Fang S, Wang Y, Jiang T. The influence of frontal lobe tumors and surgical treatment on advanced cognitive functions. *World Neurosurg*. 2016;91:340-346.
15. Solaroglu I, Beskonakli E, Kaptanoglu E, Okutan O, Ak F, Taskin Y. Transcortical-transventricular approach in colloid cysts of the third ventricle: surgical experience with 26 cases. *Neurosurg Rev*. 2004;27(2):89-92.
16. Monroy-Sosa A, Jennings J, Chakravarthi SS, et al. In reply: microsurgical anatomy of the vertical rami of the superior longitudinal fasciculus: an intraparietal sulcus dissection study. *Oper Neurosurg*. 2019;16(2):E75-E77.
17. Chakravarthi SS, Kassam AB, Fukui MB, et al. Awake surgical management of third ventricular tumors: a preliminary safety, feasibility, and clinical applications study. *Oper Neurosurg*. 2019;17(2):208-226.
18. Ribas GC. The cerebral sulci and gyri. *FOC*. 2010;28(2):208-226.
19. Ono M. M, Abernathey CD, Kubik S. *Atlas of the Cerebral Sulci*. Stuttgart: G. Thieme Verlag; New York: Thieme Medical Publishers; 1990. https://trove.nla.gov.au/version/21205667. Accessed April 9, 2019.
20. Agrawal A, Kapfhammer JP, Kress A, et al. Josef Klingler's models of white matter tracts: influences on neuroanatomy, neurosurgery, and neuroimaging. *Neurosurgery*. 2011;69(2):238-254; discussion 252-254.
21. Assistant professor, Department of Anatomy, ANIIMS, Port Blair, A&N Islands, India, patil S, sethi M, Assistant professor, Department of Anatomy, BSA Medical college and Hospital, Delhi, India, Mishra S, Director Professor & Head, Department of Anatomy, Maulana Azad medical college, New Delhi, India. Klingler's fiber dissection method- an assisting approach towards teaching neuroanatomy. *IJAR*. 2018;6(1.3):5041-5045.
22. Silva SM, Andrade JP. Neuroanatomy: the added value of the Klingler method. *Ann Anat*. 2016;208:187-193.
23. Wysiadecki G, Clarke E, Polguj M, Haładaj R, Żytkowski A, Topol M. Klingler's method of brain dissection: review of the technique including its usefulness in

practical neuroanatomy teaching, neurosurgery and neuroimaging. *Folia Morphol*. 2018;78(3):455-466.
24. Jeeves MA, Simpson DA, Geffen G. Functional consequences of the transcallosal removal of intraventricular tumours. *J Neurol Neurosurg Psychiatry*. 1979;42(2):134-142.
25. Geffen G, Walsh A, Simpson D, Jeeves M. Comparison of the effects of transcortical and transcallosal removal of intraventricular tumours. *Brain*. 1980;103(4):773-788.
26. Ribas GC, Yasuda A, Ribas EC, Nishikuni K, Rodrigues AJ. Surgical anatomy of microneurosurgical sulcal key points. *Neurosurgery*. 2006;59(4 Suppl 2):ONS177-210; discussion ONS210-211.
27. Koutsarnakis C, Liakos F, Kalyvas AV, et al. The superior frontal transsulcal approach to the anterior ventricular system: exploring the sulcal and subcortical anatomy using anatomic dissections and diffusion tensor imaging tractography. *World Neurosurg*. 2017;106:339-354.
28. Kinoshita M, de Champfleur NM, Deverdun J, Moritz-Gasser S, Herbet G, Duffau H. Role of fronto-striatal tract and frontal aslant tract in movement and speech: an axonal mapping study. *Brain Struct Funct*. 2015;220(6):3399-3412.
29. Güngör A, Baydin S, Middlebrooks EH, Tanriover N, Isler C, Rhoton AL. The white matter tracts of the cerebrum in ventricular surgery and hydrocephalus. *JNS*. 2017;126(3):945-971.
30. Baker CM, Burks JD, Briggs RG, et al. The crossed frontal aslant tract: a possible pathway involved in the recovery of supplementary motor area syndrome. *Brain Behav*. 2018;8(3):e00926.
31. Yagmurlu K, Vlasak AL, Rhoton AL. Three-dimensional topographic fiber tract anatomy of the cerebrum: *Neurosurgery*. 2015;11:274-305.

Acknowledgments

We would like to thank NICO Corporation, Carl Zeiss, Stryker Medical, and Karl Storz for their donations that made our research possible in the Neuroanatomy Laboratory.

Supplemental digital content *is available for this article at www.operativeneurosurgery-online.com*

Supplemental Digital Content. Video. Clinical case describing preoperative planning and 3D tractography modelling and operative nuances of a colloid cyst resected through the SFS Parafascicular EP.